Self-adjustment and disintegration threshold of Langmuir solitons in inhomogeneous plasmas

Y. A. Chen, Y. Nishimura,* Y. Nishida, and C. Z. Cheng
Institute of Space and Plasma Sciences, National Cheng Kung University, Tainan 70101, Taiwan
(Received 29 February 2016; revised manuscript received 22 December 2016; published 20 March 2017)

Dynamics of Langmuir solitons in the presence of a background density gradient is investigated numerically, including cases with steep gradients to the extent the solitons can disintegrate. The disintegration threshold is explained by regarding the electric field part of the soliton as a point mass moving along the self-generated potential well corresponding to the density cavity. On the other hand, it is demonstrated that the Langmuir solitons are robust when the density gradient is below the threshold. During the acceleration phase toward low density regions, Langmuir solitons adjust themselves to balance the electric field pressure and the negative plasma pressure by expelling the imbalanced portion as density cavities at the sound velocity. When the density gradient is below the disintegration threshold, the electric field part of the soliton bounces back and forth within the potential well suggesting the solitons have internal structures.

DOI: 10.1103/PhysRevE.95.033205

I. INTRODUCTION

Langmuir solitons were theoretically predicted by Zakharov [1]. In a homogeneous medium, the Langmuir solitons can propagate without changing their form when the nonlinearity from a ponderomotive force and dispersion balance. Following the theoretical prediction, Langmuir solitons were observed in a laboratory experiment via the trapping of density cavities by imposing an external radio frequency electric field [2]. In the experiment, the external electromagnetic waves underwent mode conversion to become electrostatic waves [3].

Langmuir waves are prototypical longitudinal waves in plasmas. As is often the case, whenever the wave amplitude is finite, nonlinearity comes into play. The nonlinear longitudinal waves can be retained in the form of the solitons by a coupling between the Langmuir waves and the disparate scale ion acoustic waves, which are called the Langmuir solitons. A one dimensional Langmuir soliton is known to be stable but considered to be unstable in two and three dimensional geometries [4].

In this paper, we aim at investigating whether Langmuir solitons can stably propagate in one dimensional inhomogeneous media. We then examine the mechanism of the solitons to disintegrate and discuss the threshold of *disintegration*, which we refer to as separation between the positive electric field pulse and the density cavity. The acceleration of Langmuir solitons in inhomogeneous media is studied analytically employing the nonlinear Schrödinger equation (NLSE) [5,6] and Zakharov equations [7] in a small acceleration limit and numerically at larger acceleration [8] to account for the soliton generation at a resonant density in the experiment [2]. The threshold for the survival of Langmuir solitons at large density gradients is discussed in this paper. In this paper, we employ a set of nonlinear fluid equations, the Zakharov equations, to investigate the dynamics of Langmuir solitons with inhomogeneous plasma background densities by numerical simulation, in particular, at large density gradients when the solitons can disintegrate. As predicted theoretically [5,7] and demonstrated numerically [8,9] by many other authors, the Langmuir solitons are accelerated toward the low density side. Based on the findings by numerical simulation, to explain the disintegration threshold of the solitons, we introduce the idea of quasiparticles [10], through which we interpret the acceleration as an analogy of a point mass moving along the potential well.

We also examine the emission of density cavities [11] which propagates at ion sound velocity. We would like to recall that Cow *et al.* [11] have theoretically analyzed the emission of ion sound waves by the accelerated Langmuir soliton in the limit where the velocity of the solitons is much smaller than the ion sound velocity. On the other hand, as we demonstrate below, when the density gradient is large enough to accelerate the electric field soliton (and thus gain kinetic energy) to overcome a potential energy well produced by the density cavity, the soliton can completely escape from the cavity. The density cavities will then remain as lumps without any sustaining mechanism and split into pulses propagating at the ion sound velocity. The latter sequence which separates the electric field soliton and the density cavity is what we refer to as disintegration.

This paper is organized as follows. In Sec. II, a computational model employing the Zakharov equations to describe Langmuir soliton dynamics in inhomogeneous plasmas is discussed. In Sec. III, the numerical simulation results are discussed. In Sec. IV, the disintegration threshold of Langmuir solitons with respect to the background plasma density gradient is discussed. In Sec. V, a comparison of the Zakharov simulation and the static density limit (the Zakharov equations reduce to the nonlinear Schrödinger equation) is discussed. We summarize this paper in Sec. VI.

II. COMPUTATIONAL MODEL

In this section, we discuss our computational model. As mentioned above, we solve the Zakharov equations numerically in this paper. The Zakharov equations [1,12] in the presence of density gradients [5–7] are reviewed briefly to elucidate where the dominant effect of inhomogeneous background density enters. The Zakharov equations in a one dimensional limit [12] that we employ in this paper originate

*nishimura@pssc.ncku.edu.tw

from the electron wave equation,

$$\partial_t^2 E_h - 3v_e^2\partial_x^2 E_h + \omega_e^2\left[\frac{n_{eq}(x)}{n_0}\right]E_h = -\omega_e^2\left[\frac{n}{n_0}\right]E_h, \quad (1)$$

and ion wave equation,

$$\partial_t^2 n - C_s^2\partial_x^2 n = \frac{e^2 n_0}{4\pi m_e m_i \omega_e^2}\partial_x^2|\tilde{E}|^2. \quad (2)$$

where we employed Gaussian-cgs units. Equation (1) is derived from electron fluid equations and Poisson's equation and represents the Langmuir wave dynamics with the modulation by a density change on the right side. Equation (2) is essentially the ion acoustic wave equation with the ponderomotive force on the right entering through quasineutrality. We have assumed that perturbed quantities are separated into low frequency components and high frequency components (see Ref. [12], for example). Here, E_h in Eq. (1) stands for the high frequency part of the electric field. We further set $E_h = (1/2)\tilde{E}e^{-i\omega_e t} + \text{c.c.}$, where $\tilde{E}$ is the slowly varying part of the electric field and i is the imaginary unit. Plasma frequency is given by ω_e, and $v_e = \omega_e\lambda_e$ is the electron thermal velocity (λ_e is the Debye length). In Eq. (2), n stands for the low frequency part of the plasma density, e is the unit charge, m_i and m_e are the ion and the electron masses, respectively. Note that quasineutrality is assumed for the low frequency plasma density. The background plasma density profile is given by $n_{eq}(x)$ with n_0 representing a constant density at a point in the plasma. The ion sound velocity is given by C_s.

In reaching Eqs. (1) and (2), we have also assumed that the spatial derivatives with respect to the high frequency components are larger than that for the low frequency components and similarly for the time derivatives. The inhomogeneous density enters through the third term of Eq. (1) [5–8]. In this paper, we take a linear form $n_{eq}(x) = n_0(1 - x/l)$ for the background density, where l is the characteristic length. To include the background density gradient, we have assumed that the scale length l is much larger than the soliton width. Parametrically, this latter condition is kept throughout the numerical simulation presented in this paper. As a result, the inhomogeneous background density does not appear in the ion wave equation in our model. By taking the linear form of the background density, the third term of Eq. (1) can be separated into $\omega_e^2 E_h$ and $-(\omega_e^2 x/l)E_h$. Then a part of the first term proportional to $\omega_e^2 E_h$ can be eliminated. We also assume that the magnitude of the second order time derivative $\partial_t^2\tilde{E}$ is small compared to $\omega_e\partial_t\tilde{E}$. We then find Eq. (1) of Ref. [7] and Eq. (2) of Ref. [11]. Equations (1) and (2) are equivalent to those employed in Refs. [7,8,11].

To ensure all terms are at an order of unity, in Eqs. (1) and (2), we introduce normalized quantities $T = (2\eta/3M)(\omega_e t)$ for time, $X = (2\eta^{1/2}/3M^{1/2})(x/\lambda_e)$ for length, $E = (3^{1/2}M^{1/2}/4\eta)(e\lambda_e/T_e)\tilde{E}$ for the electric field, and $N = (3M/4\eta)(n/n_0)$ for the density. Here, $M = m_i/m_e$ is the mass ratio and $\eta = M(C_s^2/v_e^2)$, which is set to unity in this paper. Then, normalized Zakharov equations in the presence of a linear background density profile are given by

$$i\,\partial_T E + \partial_X^2 E = -\alpha X E + N E, \quad (3)$$

and

$$\partial_T^2 N - \partial_X^2 N = \partial_X^2|E|^2. \quad (4)$$

As a reminder, E is the slowly varying part of the electric field, and N is the plasma density perturbation. The normalized acceleration parameter is given by $\alpha = 3M/4L$ where $L = (2\eta^{1/2}/3M^{1/2})(l/\lambda_e)$. We employ a hydrogen to electron mass ratio $M = 1836$ for numerical computations in this paper. Note that the volume integral of the electric field pressure and plasma pressure, which are the values of $\int_{-\infty}^{\infty} E^2 dX$ and $\int_{-\infty}^{\infty} N\,dX$, respectively, are conserved even when the solitons are accelerated.

The nonlinear Schrödinger type equation [13] can be obtained by assuming a static density and thus substituting $N = -|E|^2$ into Eq. (3). In the absence of inhomogeneous background density, the balance between the nonlinear drive and the wave dispersion in the NLSE sustains the soliton. Note that the nonlinearity prevails over the dispersion effects in two and three dimensional geometries and the solitons can collapse. The soliton structure shrinks, and the amplitude at the center tends to infinity at the collapse or the burn-out phase [1,4,14].

Equations (3) and (4) are time advanced numerically by the finite difference method (the leapfrog scheme instead of conventionally employed split step Fourier methods [15]) so that nonperiodic boundary conditions can be incorporated. The analytical solution is taken as the initial condition [16]. Note that Langmuir soliton solutions are parametrized by two free parameters, namely, K_0 and K_1 [1,17–19]. General solutions for the Langmuir solitons propagating at finite group velocity are given by [16,18,19]

$$E(X,T) = E_0\,\text{sech}[K_0(X - V_g T)]e^{i[K_1 X - (K_1^2 - K_0^2)T]}, \quad (5)$$

and

$$N(X,T) = -2K_0^2\,\text{sech}^2[K_0(X - V_g T)]. \quad (6)$$

Here, $E_0^2 = 2K_0^2(1 - V_g^2)$, whereas $V_g = 2K_1$ is the group velocity. Equations (5) and (6) can be obtained [18,19] by substituting the form of a traveling wave for both $E(X,T)$ and $N(X,T)$ into the Zakharov equations Eqs. (3) and (4) in the absence of the background density gradient term and solving for the real and the imaginary parts separately. The standard parameters taken are $K_0 = 3$ and $K_1 = 0$. We start from $V_g = 0$ to observe the pure acceleration mechanism. Note that the analytical solutions can be obtained only for one dimensional cases. Note also that Langmuir solitons in two and three dimensional geometries are predicted to be unstable because nonlinearity prevails over dispersion effects.

III. NUMERICAL SIMULATION RESULTS

The first numerical simulation result presented in Fig. 1 is for a Langmuir soliton with a background density change given by $L = 5 \times 10^3$. Figures 1(a) and 1(b), respectively, demonstrate acceleration [5,7,8,11] of the electric field soliton and the density cavity, whereas Fig. 1(c) shows the trace of the peak position of the density cavity measured from Figs. 1(a) and 1(b) suggesting nearly constant acceleration in the initial

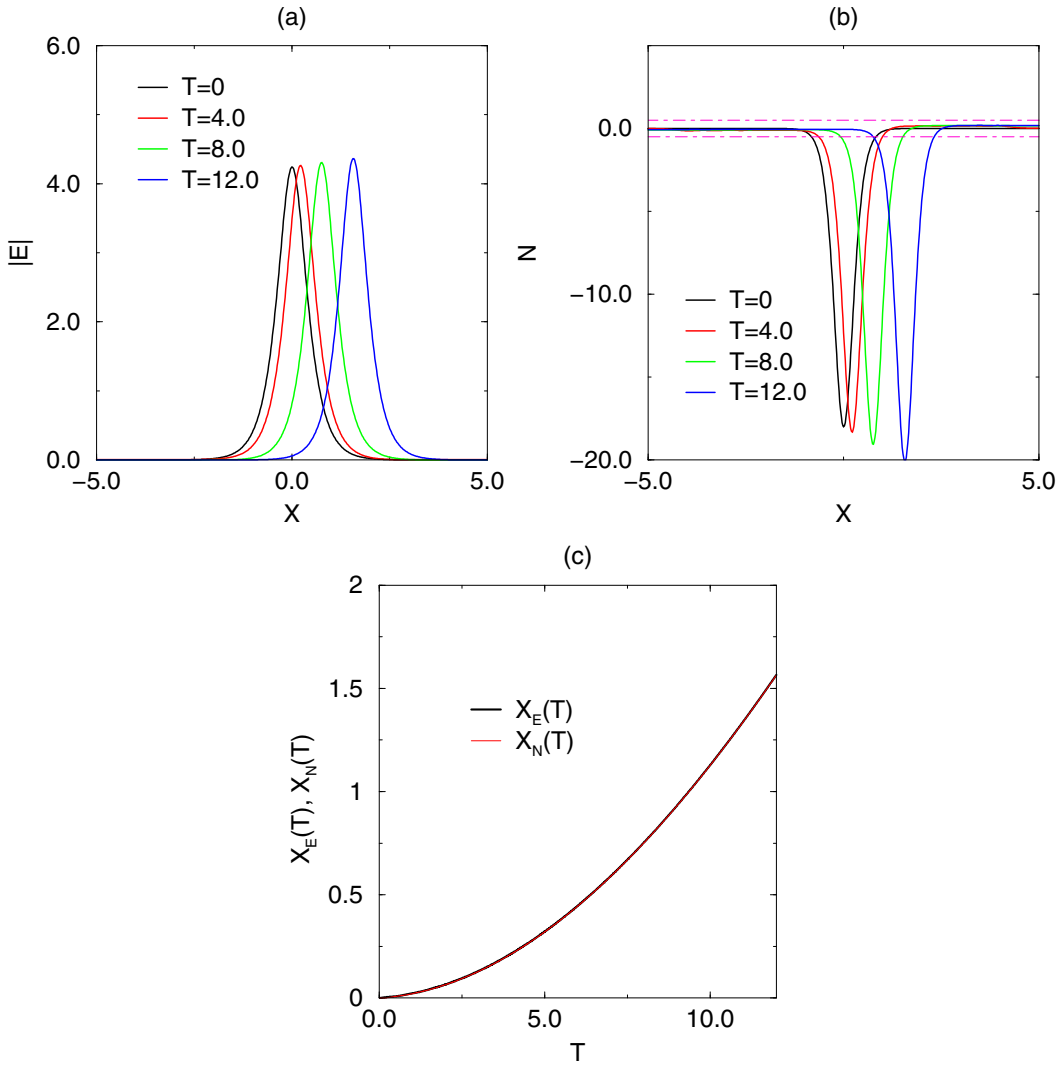

FIG. 1. Time evolution of (a) electric field soliton and (b) density cavity at $L = 5 \times 10^3$. (c) Time versus the positions of the electric field peak (X_E) and the position of density minimum (X_N).

phase when the solitons are located inside the inhomogeneous plasma. The peak positions of the electric field X_E and the positions of the density cavity minima X_N are estimated by a quadratic fitting of the solitons and the cavities because the spatial resolution is restricted by the mesh size of the finite difference method. The fitting is not in Fig. 1(c) but performed within the X space at every time step. The mesh sizes are given by $dX = 0.02$, and the time step is given by $dT = 0.2(dX)^2$ throughout this paper. The quadratic fitting allows us to accurately estimate the velocity and the acceleration of the solitons. In Fig. 1(c), initially the electric field soliton is accelerated by the theoretically estimated value of acceleration $A = 2\alpha$. However, in the case of Fig. 1, because the density cavity cannot move spontaneously and behave as a drag, the electric field soliton is decelerated (toward the negative X direction) after the acceleration and experiences oscillatory behavior within the effective potential well created by the density cavity. On average, the solitons are accelerated (toward the positive X direction) but more slowly. Note that if one takes a static density limit $N = -|E^2|$ in Eq. (3), the acceleration of the electric field soliton follows that given by theoretical prediction [5–7]. The detailed mechanism of the oscillatory behavior for small acceleration is discussed at the end of Sec. IV.

In the second case, presented in Fig. 2, we consider a shorter density scale length (meaning larger acceleration) compared to Fig. 1. Here, $L = 500$ is employed. The emission of density cavities moving exactly at the ion sound velocity is observed, the direction of which is opposite to the (electric field) soliton acceleration. It should be noted that the ion sound velocity is unity in our numerical simulation [1]. For example, local density minima of the emitted cavities are separated by a distance of 1.80 in Fig. 2(b). On the other hand, the emission of the positive density perturbation is along the direction of the soliton acceleration. Subsequent to the emission discovery, we reexamined the $L = 5 \times 10^3$ case and confirmed that the emitted density cavities (traveling at the ion sound velocity) were there as long as the acceleration was finite.

Figure 3 shows the expansion of Fig. 1(b). As we discuss at the end of Sec. IV, small ripples correspond to bounce motions of the soliton within the cavity with a distance between density minima in the range of $0.659 \leqslant \Delta X \leqslant 0.690$. In both

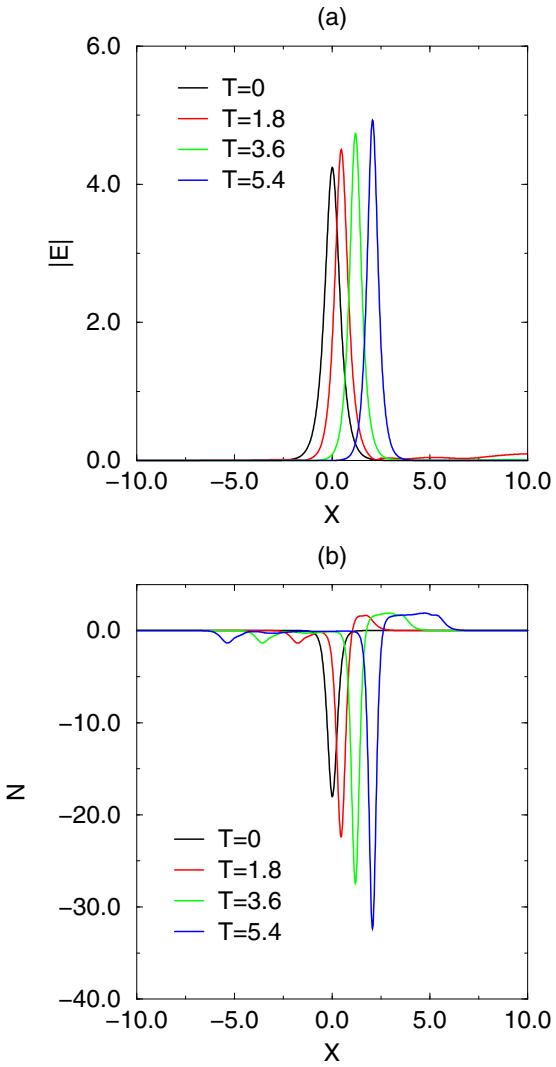

FIG. 2. Time evolution of (a) electric field soliton, and (b) density cavity at $L = 500$. Local density minima of the emitted cavities are located at $X = -5.36$ (blue curve), $X = -3.56$ (green curve), and $X = -1.76$ (red curve), which are separated by a distance of 1.80.

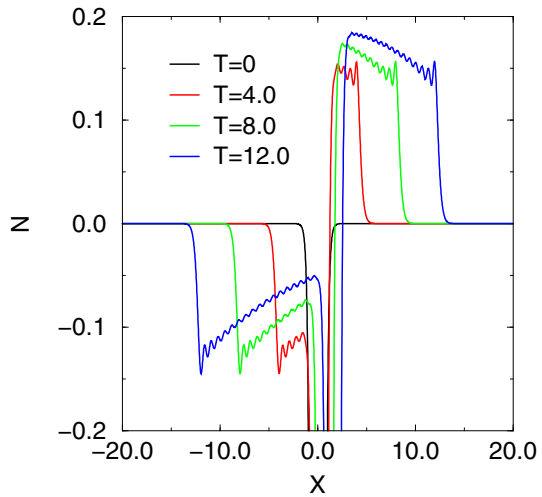

FIG. 3. An expansion of the boxed region signified by the dashed lines in Fig. 1(b).

Figs. 1 and 2, the values of $\int_{-\infty}^{\infty} E^2 dX$ and $\int_{-\infty}^{\infty} N\, dX$ still conserve to the relative error of $\leqslant 10^{-5}$. Note that isolated density cavities can be generated from any imbalance between the electric field solitons and the density cavities. For example, if we set mismatched initial conditions in Eqs. (3) and (4) (i.e., whenever the balance between the electric field pressure and the plasma pressure by the density cavity breaks), one can still observe the cavity emission. The plasma inhomogeneity, however, is one of the ubiquitous ingredients of the balance breaking.

We now take an even shorter density scale length of $L = 50$. For a plasma with an electron temperature of 1 eV and a density of 10^{10} cm^{-3}, $L = 50$ corresponds to 24 cm (the soliton's full width at half maximum is approximately 0.14 cm with $K_0 = 3.0$). With a further increase in the density gradient, we observe the solitons disintegrate. The electric field quickly spreads with the density inhomogeneity above the threshold, and the density cavity loses its sustaining mechanism by the ponderomotive force. In the absence of the sustaining electric field, the original density cavity splits into two lumps (which then propagate in opposite directions at the ion sound velocity). Note that the density lumps are both negative, which is in contrast to the subsonic acceleration cases of Figs. 1 and 2 (one being a cavity, and the other being a positive density perturbation). Here in Fig. 4, a numerical simulation domain of $-20 \leqslant X \leqslant 60$ is prepared beforehand to incorporate the rapid spread of the electric field.

IV. DISINTEGRATION THRESHOLD OF LANGMUIR SOLITONS

The disintegration of the soliton at the large density gradient limit can be understood by comparing the first Zakharov equation, which has the form of a Schrödinger type equation, to a one dimensional Hamiltonian of a particle with momentum P in a potential $V(X)$,

$$H(P,X) = P^2/2 + V(X).$$

From a mathematical analogy, in comparison with the Hamiltonian, the first term in Eq. (3) corresponds to the kinetic energy (except for the factor 1/2), and the terms on the right side of Eq. (3) correspond to potential $V(X) \leftrightarrow N - \alpha X$. As a reminder, the idea bridging between the Schrödinger type equation and a particle motion is that of matter waves [20]. We also note that for a nonlinear Schrödinger equation [which we obtain by considering the static density limit and substituting $N = -|E^2|$ into Eq. (3)], by introducing the idea of a pseudopotential [12,21,22], both the value of E and its first derivative tend to zero at $X \to \pm\infty$. One can find a spatially localized solution suggesting existence of solitons.

Without the nonlinearity, the point mass (soliton) moves down along the potential (density) well, toward the positive X direction in the cases of Figs. 1–4. Figure 5(a) shows the concept of the soliton moving subject to the potential (which is referred to as a quasiparticle [10]). For the matter wave, $|E|^2 dX$ is proportional to the probability of a point mass found within a small volume dX [20]. Complimentary to finding the peak position of the electric field X_E, we trace the center of gravity of the E^2 profile to determine the position of the quasiparticle. At each time step, we can find the center of

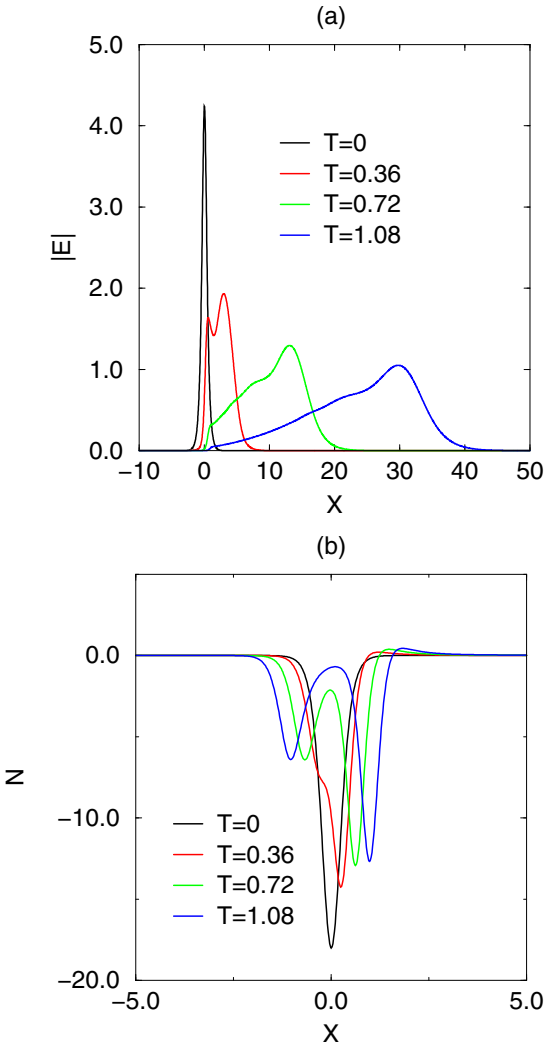

FIG. 4. Time evolution of (a) electric field soliton, and (b) density cavity at $L = 50$. Disintegration of the Langmuir solitons caused by a quick escape of the electric field soliton.

gravity X_{EC} which satisfies the relation,

$$\int_{-\infty}^{X_{EC}} E^2 dX = \frac{1}{2}\int_{-\infty}^{\infty} E^2 dX. \tag{7}$$

Figure 5(b) compares the spread of the electric field in the cases with (solid curves) and without (dashed curves) the nonlinear term in Eq. (3). Correspondingly, Fig. 5(c) shows the center of gravity X_{EC} versus time for the two cases. By observing the two cases in Figs. 5(b) and 5(c), it can be known that the linear potential term dominates the electric field dynamics when $L = 50$. From a plasma physics point of view [23], the acceleration is due to the restoring force in plasma oscillation being larger toward the lower density side compared to toward the higher density side.

The acceleration threshold (the threshold density gradient) for the soliton disintegration is considered. From the particle motion's analogy, the condition of the kinetic energy being larger than the potential energy provides us with $V^2/2 = AW{=}N$ as a threshold. Here, W signifies the soliton width

TABLE I. A comparison of numerically estimated threshold values of L and analytically estimated threshold values. For different K_0 values employed in Fig. 6.

K_0	1.0	1.5	2.0	2.5	3.0	3.5	4.0
L (analytical)	2065	612.0	258.2	132.2	76.50	48.17	32.27
L (numerical)	1325	530	265	150	90	57	37

(see the Appendix). For example, from the potential depth of $N = 2K_0^2 = 18$ and the soliton width of $W = 0.5$, we estimate a required acceleration of $A = 36$ or $L = 76.5$ for an escape and thus disintegration of the soliton. Since the function $\mathrm{sech}^2(K_0 X)$ has an infinitely long tail, we need to set a finite width to tell ourselves if the majority of the electric field soliton has escaped from the potential well made by the density cavity. In this paper, we set the soliton width at $K_0 W = 1.5$ where the integrated area occupies approximately 90.5% of $\int_{-\infty}^{\infty} E^2 dX$.

Figure 6 and Table I summarize the numerically measured values of K_0 versus the solitons' disintegration threshold L with $K_1 = 0$. The solid curve in Fig. 6 is given analytically by Eq. (A4). The way we numerically estimated the disintegration thresholds in L is as follows. By finding the position X_N of the density's minimum, we estimate the area $S_1 = \int_{X_N - W}^{X_N + W} E^2 dX$, where $W = 1.5/K_0$. At $T = 0$, S_1 includes 90.5% of the whole area $S_0 = \int_{-\infty}^{\infty} E^2 dX = 4K_0$. During the time evolution of the solitons, if the value S_1/S_0 ever becomes less than 1%, we regard the soliton to be disintegrated. We also impose the condition that the propagation distance of the soliton should not exceed the characteristic length L.

In Fig. 6, we see a tendency for the threshold L values being smaller than the analytical values for small K_0 values ($K_0 \leqslant 2$ for wider solitons). The discrepancies in the smaller K_0 region as we understand from our observation is due to the displacement of the density cavity toward positive X directions during the acceleration phase of electric field soliton. As a reminder, we assumed the density cavity to be fixed in space in deriving our estimation (see the Appendix). On the other hand, the measured threshold L values are slightly larger than the analytical values for large K_0 values ($K_0 \geqslant 2$). This is because, for the larger K_0 values, the density cavity separates into dominant two lumps in a relatively short time [see Fig. 4(b), for example] and the effective potential depth is reduced. Despite finite discrepancies, we believe our model formula (based on the idea of point mass trapped in a potential well) has captured certain aspects of the disintegration threshold. Based on the supporting findings in Fig. 6, we would like to understand that the mechanism of the soliton disintegration is due to the electric field soliton overcoming the density cavity's potential.

Large amplitude nonlinear Alfvén waves can induce particle acceleration along the magnetic field and thus density compression. Similar to the Zakharov system, the nonlinear Alfvén waves [24–26] when they are coupled to ion acoustic waves can be described by a derivative nonlinear Schrödinger equation [25,26] in a static density limit. The Alfvén soliton's collapse threshold by modulational instabilities is investigated numerically and analytically [26–28]. By introducing the idea

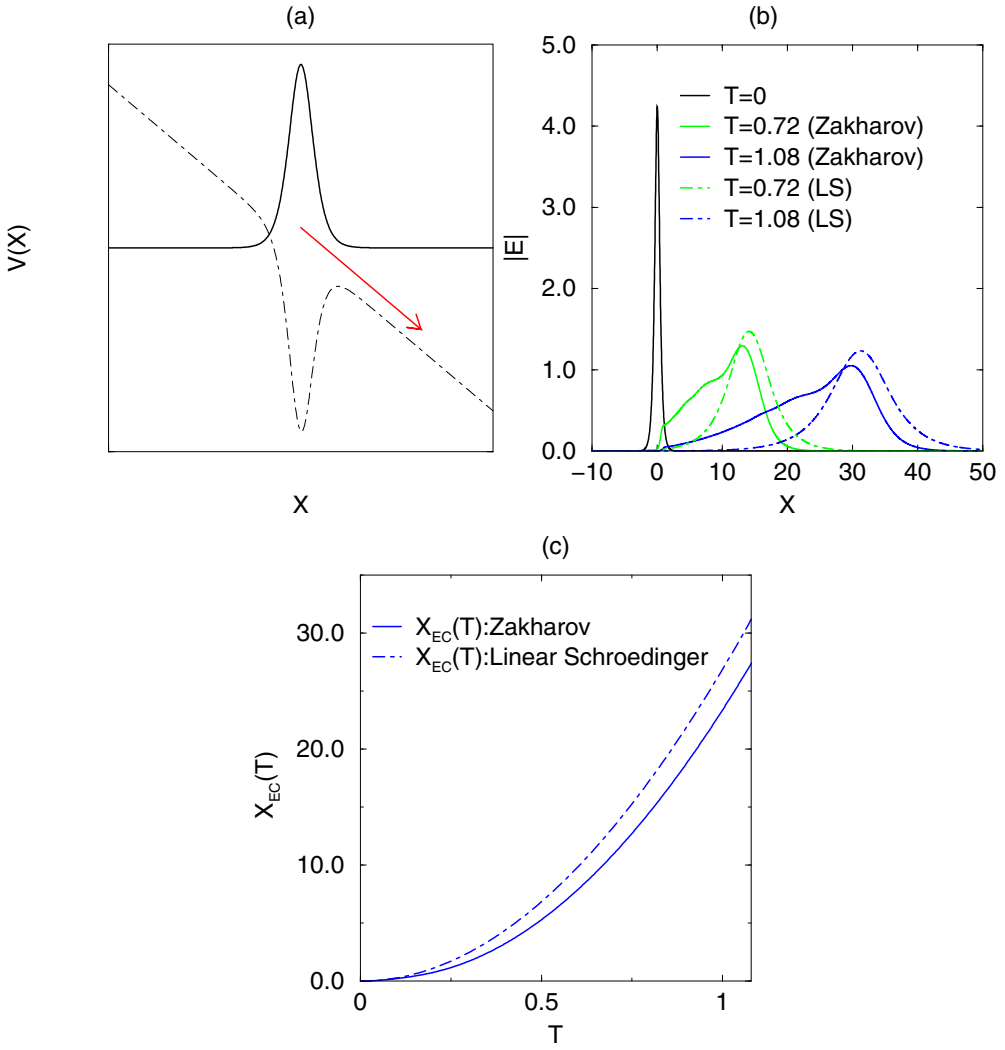

FIG. 5. Disintegration of solitons at a high density gradient. (a) Conceptual figure of a soliton being regarded as a particle falling down toward the right under potential $V(X)$ given by a superposition of a linearly varying function and a cavity. (b) Spread of the electric field soliton compared with the solution of a linear Schrödinger equation. Here, LS stands for linear Schrödinger. (c) The center of gravity X_{EC} of the electric field soliton versus time for the two cases. The solid curve is obtained from the solution from the Zakharov equations, and the dashed curve is obtained from the solution of the linear Schrödinger equation.

of a time scale for a change in the wave field intensity (τ_1) and the time scale for an ion acoustic wave to propagate across the soliton (τ_2), Spangler [28] has discussed a condition for the static approximation to be valid for the Alfvén solitons. Employing the two time scales, the static approximation is valid when $\tau_1 \gg \tau_2$, which reads $\varepsilon = W(\partial_t|E^2|)/|E^2| \ll 1$ in our studies. In our study of Zakharov equations, the change in the wave field intensity is induced by inhomogeneous background density. For a static approximation to be valid for us in the presence of the density inhomogeneity, a formula is suggested [28] in the form of

$$\frac{L}{V} \gg \frac{W}{|\bar{C}_s - V|}, \tag{8}$$

where V is the group velocity of the solitons and $\bar{C}_s$ ($= 1$ in our normalization) is the normalized ion sound velocity. Applying $\varepsilon \to 1$, antithetical to the idea of the static approximation, we obtain $V \simeq 1$, which means, if the velocity of the Langmuir solitons immediately becomes close to the ion sound wave velocity, solitons can disintegrate. This is consistent with our finding from the numerical simulation of Fig. 4.

Contrary to the disintegrating limits with large density gradients, if the remaining electric field or the quasiparticle is still trapped in the density cavity, it will oscillate within the well. A signature of the soliton bounce motion (mismatch of the peak positions) in the potential well is suggested in Fig. 7 for a small density gradient case (obtained from the same simulation in Fig. 1 at $L = 5000$). Figure 7 shows the velocity of the peak position of the electric field soliton ($V_E = dX_E/dT$) and the velocity of the density minimum position ($V_N = dX_N/dT$). The period of bounce motion in the initial phase is in the range of $0.668 \leqslant \Delta T \leqslant 0.681$, which is correlated with the distances between density minima (in the range of $0.659 \leqslant \Delta X \leqslant 0.690$) estimated in Fig. 3. As a reminder, the ion sound velocity is unity in our normalization.

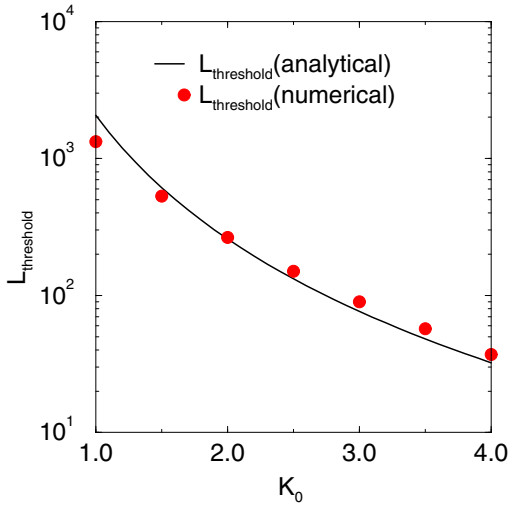

FIG. 6. Values of the solitons' disintegration threshold L versus the soliton shape parameter K_0. Here we set $K_1 = 0$, and thus the initial velocity of the solitons is zero. The solid black curve is given by an analytical estimate $L = 3MW/(2K_0)^2$ (see the Appendix). Numerically measured values are given by red circles.

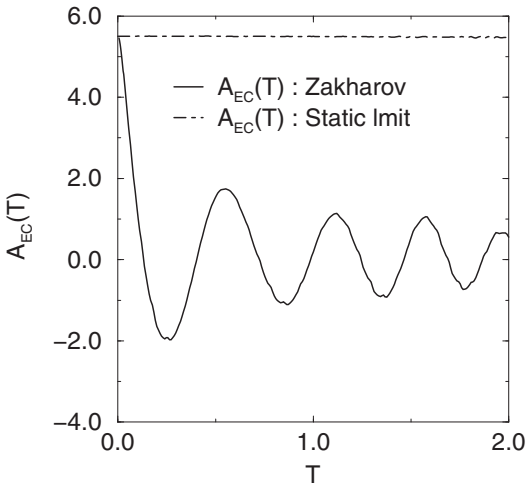

FIG. 8. The acceleration of the center of gravity of the electric field soliton (A_{EC}) for the $L = 500$ case of Fig. 2. The solid curve is obtained from simulation by the Zakharov equation, whereas the dashed curve is from the static density limit.

V. SOLITON ACCELERATION IN THE STATIC DENSITY LIMIT

A comparison with a static density limit ($N = -|E|^2$) is discussed. In the Zakharov system, due to the trapping of the electric field by the cavity, the acceleration is small compared to the NLSE limit [5]. In Fig. 8, we take a second order time derivative of the center of gravity $A_{EC} = d^2X_{EC}/dT^2$ to estimate the acceleration. Although the acceleration is constant for the NLSE case, much smaller values of acceleration are found in the Zakharov system. Taking the $L = 500$ case of Fig. 2 as an example, the acceleration of the Zakharov soliton is not constant; rather it is time dependent as shown in Fig. 8, whereas $5.43 \leqslant A_{EC} \leqslant 5.51$ for the static density limit (NLSE limit), being close to the theoretically predicted value of $A = 2\alpha = 5.508$ [5]. This is because the density cavity cannot move faster than the ion sound velocity and hinder the electric field soliton unless it can completely escape within the first bounce motion as in the Fig. 4 case. If we solve the NLSE with the same parameter and the same initial condition in Eq. (4), the solitons do not decay simply because they do not have emission of the density cavities as in the Zakharov system.

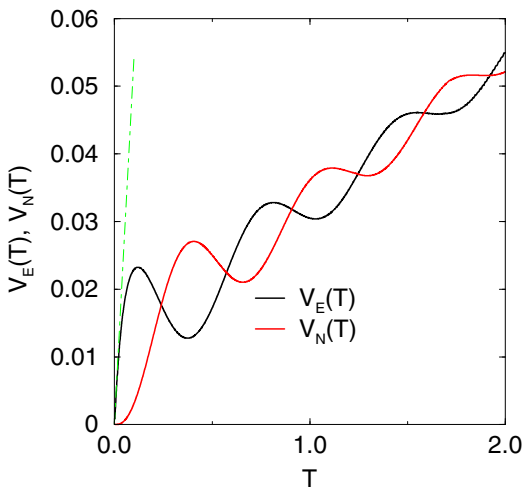

FIG. 7. Demonstration of the mismatch between the velocity of the peak position of the electric field soliton (V_E) and the velocity of the density minimum position (V_N) for the $L = 5 \times 10^3$ case of Fig. 1. The green dashed line is a tangent line to the soliton velocity in the very initial phase. If a static density limit ($N = -|E|^2$) is taken, the velocity of the electric field soliton should obey the green dashed line all the way. In practice, they cannot due to a dragging effect by the density cavity, however.

VI. SUMMARY AND DISCUSSIONS

To summarize, the Langmuir soliton dynamics in inhomogeneous plasmas was investigated numerically. By a series of numerical simulations solving Zakharov equations, we have recovered the feature of the solitons being accelerated toward the low density side as predicted theoretically in Refs. [5–7,11] and demonstrated in Refs. [8,9]. As a consequence of the acceleration and thus a mismatch between the electric field solitons and the density cavities, isolated cavities moving exactly at the ion sound velocity are emitted [11]. When the acceleration is further increased, solitons disintegrate, and the density cavities split into two lumps released also at the ion sound velocity. The disintegration threshold is estimated by an analogy between the soliton and a particle overcoming the self-generated potential well.

The current paper considered nonlinear wave-wave interactions through Zakharov's fluid model. In the future, we plan to conduct numerical computations by Vlasov simulation [29,30] to incorporate wave-particle interaction to investigate a much more realistic mechanism of the Langmuir soliton's sustainment and disintegration.

ACKNOWLEDGMENTS

One of the authors (Y.N.) would like to acknowledge discussions with Professor P. K. Kaw during his visit to Taiwan. This work was supported by Taiwan NSC Grant No. 100-2112-M-006-021-MY3, Taiwan MOST Grant No. 103-2112-M-006-007, and Taiwan MOST Grant No. 104-2112-M-006-019.

APPENDIX: ESTIMATION OF THE DISINTEGRATION THRESHOLD

Here, we would like to estimate the soliton's disintegration threshold based on energy conservation of quasiparticles. We assume that the solitons do not have an initial group velocity. Assuming the density cavity has moved W within a time duration T under acceleration A, we obtain

$$\frac{AT^2}{2} = W, \tag{A1}$$

where W corresponds to the soliton width. If the effective kinetic energy of the soliton is fully converted into the potential energy whose magnitude is given by the density cavity $N = 2K_0^2$, we obtain

$$\frac{V^2}{2} = N = 2K_0^2, \tag{A2}$$

where $V = AT$. From Eqs. (A1) and (A2) we obtain the threshold acceleration,

$$A = \frac{(2K_0)^2}{2W} \tag{A3}$$

to disintegrate the solitons. Because $A = 3M/2L$, the threshold density length scale can be given by

$$L = \frac{3MW}{(2K_0)^2}. \tag{A4}$$

The black solid curve in Fig. 6 is given by varying K_0 in the last expression.

[1] V. E. Zakharov, Sov. Phys. JETP **35**, 908 (1972).
[2] H. C. Kim, R. L. Stenzel, and A. Y. Wong, Phys. Rev. Lett. **33**, 886 (1974).
[3] R. L. Stenzel, A. Y. Wong, and H. C. Kim, Phys. Rev. Lett. **32**, 654 (1974).
[4] L. Bergé, Phys. Rep. **303**, 259 (1998).
[5] H. H. Chen and C. S. Liu, Phys. Rev. Lett. **37**, 693 (1976).
[6] H. H. Chen and C. S. Liu, Phys. Fluids **21**, 377 (1978).
[7] K. V. Chukbar and V. V. Yankov, Sov. J. Plasma Phys. **3**, 780 (1977).
[8] G. J. Morales and Y. C. Lee, Phys. Fluids **20**, 1135 (1977).
[9] B. Eliasson and B. Thide, J. Geophys. Res. **113**, A02313 (2008).
[10] L. D. Landau, Sov. Phys. JETP **3**, 920 (1957).
[11] P. K. Cow, N. L. Tsintsadze, and D. D. Tskhakaya, Sov. Phys. JETP **55**, 839 (1982).
[12] D. R. Nicholson, *Introduction to Plasma Theory* (Wiley, Hoboken, NJ, 1983), p. 177.
[13] V. L. Ginzburg and L. D. Landau, Zh. Eksp. Teor. Fiz. **20**, 1064 (1950).
[14] M. V. Goldman, Rev. Mod. Phys. **56**, 709 (1984).
[15] T. R. Taha and M. I. Ablowitz, J. Comput. Phys. **55**, 203 (1984).
[16] N. R. Pereira, R. N. Sudan, and J. Denavit, Phys. Fluids **20**, 271 (1977).
[17] V. E. Zakharov and A. B. Shabat, Sov. Phys. JETP **34**, 62 (1972).
[18] L. I. Rudakov, Dokl. Akad. Nauk SSSR **207**, 821 (1972).
[19] L. M. Degtyarev, V. G. Nakhan'kov, and L. I. Rudakov, Sov. Phys. JETP **40**, 264 (1975).
[20] L. I. Schiff, *Quantum Mechanics* (McGraw-Hill, New York, 1955), p. 23.
[21] P. J. Hansen and D. R. Nicholson, Am. J. Phys. **47**, 769 (1979).
[22] R. Z. Sagdeev, *Reviews of Plasma Physics* (Consultants Bureau, New York, 1966), Vol. 4, p. 23.
[23] J. M. Dawson, Phys. Rev. **113**, 383 (1959).
[24] A. Hasegawa, Phys. Fluids **15**, 870 (1972).
[25] K. Mio, T. Ogino, K. Minami, and S. Takeda, J. Phys. Soc. Jpn. **41**, 265 (1976).
[26] S. R. Spangler and J. P. Sheerin, J. Plasma Phys. **27**, 193 (1982).
[27] S. R. Spangler, Astrophys. J. **299**, 122 (1985).
[28] S. R. Spangler, Phys. Fluids **30**, 1104 (1987).
[29] C. Z. Cheng and G. Knorr, J. Comput. Phys. **22**, 330 (1976).
[30] Y.-H. Chen, Y. Nishimura, and C.-Z. Cheng, Terres. Atmos. Ocean. Sci. **24**, 273 (2013).